Salt-Dependent DNA Superhelix Diameter Studied by Small Angle Neutron Scattering Measurements and Monte Carlo Simulations

Markus Hammermann,* Nathalie Brun,* Konstantin V. Klenin,* Roland May,# Katalin Tóth,* and Jörg Langowski§

*Biophysics of Macromolecules Division, German Cancer Research Center, Im Neuenheimer Feld 280, D-69120 Heidelberg, Germany and #ILL Grenoble, Avenue des Martyrs, BP156, F-38042 Grenoble Cedex 9, France

ABSTRACT Using small angle neutron scattering we have measured the static form factor of two different superhelical DNAs, p1868 (1868 bp) and pUC18 (2686 bp), in dilute aqueous solution at salt concentrations between 0 and 1.5 M Na^+ in 10 mM Tris at 0% and 100% D_2O. For both DNA molecules, the theoretical static form factor was also calculated from an ensemble of Monte Carlo configurations generated by a previously described model. Simulated and measured form factors of both DNAs showed the same behavior between 10 and 100 mM salt concentration: An undulation in the scattering curve at a momentum transfer $q = 0.5$ nm^{-1} present at lower concentration disappears above 100 mM. The position of the undulation corresponds to a distance of ~10–20 nm. This indicated a change in the DNA superhelix diameter, as the undulation is not present in the scattering curve of the relaxed DNA. From the measured scattering curves of superhelical DNA we estimated the superhelix diameter as a function of Na^+ concentration by a quantitative comparison with the scattering curve of relaxed DNA. The ratio of the scattering curves of superhelical and relaxed DNA is very similar to the form factor of a pair of point scatterers. We concluded that the distance of this pair corresponds to the interstrand separation in the superhelix. The computed superhelix diameter of 16.0 ± 0.9 nm at 10 mM decreased to 9.0 ± 0.7 nm at 100 mM salt concentration. Measured and simulated scattering curves agreed almost quantitatively, therefore we also calculated the superhelix diameter from the simulated conformations. It decreased from 18.0 ± 1.5 nm at 10 mM to 9.4 ± 1.5 nm at 100 mM salt concentration. This value did not significantly change to lower values at higher Na^+ concentration, in agreement with results obtained by electron microscopy, scanning force microscopy imaging in aqueous solution, and recent MC simulations, but in contrast to the observation of a lateral collapse of the DNA superhelix as indicated by cryo-electron microscopy studies.

INTRODUCTION

Beyond the primary DNA sequence of the genome, which is becoming available for more and more organisms, the three-dimensional folding of the DNA in the cell determines its function to a large extent. An important "folded state" of DNA is the superhelix, which is formed when a piece of DNA is put under torsional stress, e.g., during translation or replication (Bates and Maxwell, 1993). Here the DNA double strand is wound around itself such that segments that are far from each other on the primary sequence can come into close neighborhood. Such long-range interactions are important, e.g., in gene regulation by enhancer-promoter interaction (Rippe et al., 1997a). In order to understand how superhelicity can control such processes it is important to understand the structure of the superhelix and its changes in different environments. To study the structure of superhelical DNA, imaging techniques like electron microscopy, cryo-electron microscopy, and scanning force microscopy have been successfully used for imaging of single molecules. However, any technique in which a flexible molecule like DNA is bound to a surface or confined to a rigid matrix can create artifacts. Furthermore, the only way to compute conformational statistics for a large number of molecules is to evaluate individual images, which can be tedious. To quantify structural properties of DNA free in solution under noninvasive conditions, methods such as analytical ultracentrifugation or static and dynamic light scattering have been used widely (Schurr, 1977; Langowski et al., 1986; Langowski, 1987; Langowski and Giesen, 1989; Rybenkov et al., 1997). The drawback with such techniques is that the structural information gained is *a priori* not very detailed; typically, some simple quantities such as diffusion or sedimentation coefficient, a scattering curve or parameters indirectly related to the dynamics of the molecule are obtained. For interpreting these measured quantities, models therefore have to be used. In particular, Monte Carlo and Brownian dynamics simulations served to interpret hydrodynamic and solution scattering data of DNA (Klenin et al., 1991, 1995; Vologodskii et al., 1992; Kremer et al., 1993; Bednar et al., 1994; Langowski et al., 1994; Gebe et al., 1995, 1996; Hammermann et al., 1997; Rybenkov et al., 1997). From the models it was also possible to compute parameters which are important during transcriptional activation, such as cyclization probabilities mediated by proteins or end-to-end collisions frequencies of short DNA fragments with a permanent bend (Merlitz et al., 1998).

The quality of these DNA simulation programs makes it now possible to predict effects which have not yet been observed in measurements. Monte Carlo simulations of superhelical DNA solution scattering predicted a modulation in the scattering form factor at a scattering vector

Received for publication 10 April 1998 and in final form 9 September 1998.

Address reprint requests to Dr. Jörg Langowski, Deutsches Krebsforschungszentrum, Abt. Biophysik der Makromolekule (0830), Postfach 101949, D-69009 Heidelberg, Germany. Tel.: 49-6221-423390; Fax: 49-6221-423391; E-mail: joerg.langowski@dkfz-heidelberg.de.

0006-3495/98/12/3057/07 $2.00

modulus $q \approx 0.5\ \mathrm{nm}^{-1}$ which shifts to higher values with increasing ionic strength. We show in the following that this modulation and its salt dependence can be verified experimentally by small angle neutron scattering on superhelical DNA of 1868 and 2686 bp. From the modeled conformations we could then determine the superhelix diameter of DNA in aqueous solution over a wide range of Na^+ concentrations. A similar salt effect had been observed in earlier x-ray scattering studies by Brady et al. (1987), but the authors interpreted the change as only being consistent with a non-interwound form of the superhelix. Here, the comparison with the simulations clearly demonstrates that the salt effect can be explained by a change in the interstrand separation in the DNA superhelix in an interwound form.

These results are of particular relevance, since recently attention has focused on the interaction between opposing double strands in an interwound superhelix and its modulation by the counterion concentration. Bednar et al. (1994) observed in cryo-electron microscopy studies a lateral collapse of the interwound structure for Na^+ concentrations >0.1 M or at millimolar concentrations of Mg^{2+}. The relevance of this observation for the solution structure of the superhelix has been put in question by recent results of Gebe et al. (1996), who could not find evidence for such a collapse in static and dynamic light scattering, fluorescence polarization anisotropy decay, or circular dichroism measurements. In another recent study, a comparison of sedimentation coefficients of superhelical DNA as determined by analytical ultracentrifugation and as calculated from Monte Carlo simulations gave a consistent description of the salt-dependent solution structure of the DNA (Rybenkov et al., 1997). This model could predict the superhelix diameter, and no collapse up to 1 M was found.

Our neutron scattering measurements shown here give a direct measure of the superhelix diameter and do not show evidence for a collapse at Na^+ concentrations up to 1.5 M. They are in agreement with the results mentioned above and with recent scanning force microscopy images supporting a superhelix diameter of not less than 10 nm even in the presence of 10 mM Mg^{2+} (Rippe et al., 1997b).

MATERIALS AND METHODS

Superhelical DNA preparation

pUC18 plasmid DNA (2868 bp) was prepared from *Escherichia coli* HB 101 as described (Kapp and Langowski, 1992; Langowski, 1987), p1868 (1868 bp) was prepared as described (Hammermann et al., 1997). After ethanol precipitation and short drying the crude DNA was dissolved in TE buffer (10 mM Tris-HCl, pH 7.5, 1 mM EDTA). For additional purification and concentration the DNA was precipitated for 15 h on ice by adding a 50% solution of PEG 20000 in 0.5 M NaCl to a final PEG concentration of 10% in 0.6 M NaCl. The DNA was pelleted at 8000 rpm and 4°C in the HB4 rotor in a Sorvall RC-5B centrifuge and again dissolved in TE buffer. Supercoiled and relaxed plasmids were separated by HPLC as described (Kapp and Langowski, 1992). The integrity of the DNA plasmids and the superhelical density was checked by agarose gel electrophoresis (1%) in Tris-acetate buffer (40 mM Tris-acetate, 2 mM EDTA, pH 8). Only samples containing more than 90% supercoiled DNA were used for neutron scattering measurements in 10 mM Tris-HCl, 0.1 mM EDTA, pH 7.5 with varying amounts of NaCl. As a control, scattering functions of relaxed plasmids were also collected. The NaCl concentration was varied between 0 and 1.5 M and controlled by conductivity measurements. DNA concentrations were 2–6 mg/ml. Both plasmids were also dialyzed against the same buffer with 100% D_2O, dialysis was performed in 100× sample volume in Sartorius collodium bags (cellulose nitrate, 12000 D MWCO, FRG) with at least three buffer changes.

Neutron scattering measurements

Measurements were performed at the D22 large scale structure diffractometer at the Institut Laue-Langevin (ILL), Grenoble (Ibel, 1994). The sample cuvette (quartz, 1 mm light path, $7 \times 10\ \mathrm{mm}^2$ illuminated cross-section, Hellma GmbH, Müllheim, FRG) was thermostatted at 20°C. The neutron wavelength was 8 Å, the sample detector distance was set to 5.0 or 2.5 m to reach a momentum transfer q range of 0.1–3 nm^{-1}. Data were collected for at least 1–2 h at each Na^+ concentration. After radial integration the data were corrected for sample transmission at 0 and 100% D_2O. Background and buffer scattering were subtracted. For comparison of data sets at different sample concentrations and slight baseline deviations in the D_2O samples, the data were renormalized to the same intensity at low q and the baseline at high q was corrected to the same value.

DNA simulations

The conformations of p1868 and pUC18 were simulated by use of a Monte Carlo algorithm originally developed by Vologodskii et al. (1992). The algorithm is now part of a combined Brownian dynamics and Monte Carlo simulation program implemented in C++. The details of the Brownian dynamics procedure have recently been published (Klenin et al., 1998). The elastic and electrostatic potentials are the same for both Brownian dynamics and Monte Carlo simulations. The DNA was divided into 64 (p1868) and 91 (pUC18) segments of 10.0 nm length corresponding to 29.4 bp. Since this size is significantly smaller than the persistence length (assumed here 50 nm), the individual segments can be regarded as rigid rods. We used a Kuhn statistical length of 100 nm independent of Na^+ concentration (Hagerman, 1988), and a torsional rigidity constant $C = 2 \cdot 10^{-19}$ erg cm (Schurr et al., 1992). The electrostatic energy is the expression for the energy of interaction between two uniformly charged nonadjacent segments (i, j) in the Debye-Hückel approximation:

$$\frac{E_{ij}^{(e)}}{k_B T} = \frac{\nu^2}{k_B T D} \int d\lambda_i \int d\lambda_j \frac{\exp(-\kappa r_{ij})}{r_{ij}}. \qquad (1)$$

The integration is done along the two segments, λ_i and λ_j are the distances from the segment beginnings, r_{ij} is the distance between the current positions at the segments to which the integration parameters λ_i and λ_j correspond; κ is the inverse of the Debye length, so that $\kappa^2 = 8\pi e^2 I / k_B T D$, I is the ionic strength, e the proton charge, D the dielectric constant of water, ν the linear charge density which for DNA is equal to $\nu_{DNA} = -2e/\Delta$, where $\Delta = 0.34$ nm is the distance between two base pairs. To ensure the correct excluded volume effects, the renormalization of the linear density was done as in Stigter (1977). As pointed out in Schellman and Stigter (1977), the Gouy layer of immobile counterions reduces the effective charge density by a factor of $q = 0.73$ for NaCl concentrations between 1 and 500 mM. Next, the Debye-Hückel approximation is a linearization of the Poisson-Boltzmann equation and valid only for a very small electric potential: $\varphi \ll k_B T/e$. We chose the renormalized charge density ν^* in such a way that the known solution of the Debye-Hückel equation for a straight thin line with charge density ν^* coincides with the solution of the Poisson-Boltzmann equation for a cylinder of the DNA radius r_{ES} and the charge density $q\nu_{DNA}$ in the regions where $\varphi \ll k_B T/e$.

The Monte Carlo steps used were exclusively rotational "pivot" moves where parts of the chain were rotated against one another, other than in the

original publication (Vologodskii et al., 1992), where reptational and rotational moves were used. The deficit linking number in the simulations was set to the native value measured for each plasmid in gel electrophoresis buffer, $\Delta Lk = -9$ for p1868 and $\Delta Lk = -13$ for pUC18. These values were not varied for the simulations at different Na^+ concentrations. As a control, the relaxed form of both plasmids was also simulated by setting $\Delta Lk = 0$. All simulations were done assuming a temperature of $T = 20°$, starting from a flat circle as initial configuration. 10^6 simulation steps were done and the last configuration was taken as new starting configuration. Another $9 \cdot 10^6$ steps were calculated, each 1000th configuration was saved to a final set of 9000 configurations for each Na^+ concentration.

To calculate static scattering functions from the saved configurations, each segment was divided into four smaller segments of 2.5 nm length to minimize the influence of the segment length on the distance distribution. The total segment number was then 256 for p1868 and 364 for pUC18. A further division of the 2.5-nm segments into 1.25-nm segments had no significant influence on the distance distribution of the segments. The static form factor was calculated and averaged over all configurations and orientations of the macromolecules according to Debye (1915),

$$P(q) = \frac{1}{N^2} \sum_{i=1}^{N} \sum_{j=1}^{N} \frac{\sin(q|\vec{r}_i - \vec{r}_j|)}{q|\vec{r}_i - \vec{r}_j|} \quad (2)$$

where q is the momentum transfer, N the number of segments, and $\vec{r}_i$ and $\vec{r}_j$ the positions of the segments i and j. $P(q)$ was multiplied by a constant K to fit the experimental data $I(q)$, a constant term was added to fit the measured baseline at high q. To quantify the superhelix diameter, we calculated the average distribution function $p(r)$ of the distance between each segment pair $\vec{r}_i$ and $\vec{r}_j$,

$$p(r) = \langle p(|\vec{r}_i - \vec{r}_j|) \rangle \quad (3)$$

Additionally, we calculated the average distribution function $p_n(r)$ of each segment $\vec{r}_i$ and its nearest opposite neighbor $\vec{r}_j$ with the constraint that the two segments are separated by at least 10 segments along the chain:

$$p_n(r) = \langle p(|\vec{r}_i - \vec{r}_j|) \rangle \quad (4)$$

The meaning of this quantity is illustrated in Fig. 1. Opposing segments are connected by a straight line. Segment pairs 2–4 are nearest neighbors and therefore a measure of the superhelix diameter. A segment in an end loop finds its counterpart at a larger distance (pair 1) because the segments are separated by 10 segments along the chain. The number 10 was chosen arbitrarily; there was no significant influence of this number on the peak in the distribution above a lower limit of approximately five segments separation along the chain. Segments located in end loops will give rise to a long tail in the distribution $p_n(r)$. However, only a small number of segments are located in end loops; thus, a peak in $p_n(r)$ can be regarded as average diameter of interwound regions of the plasmid.

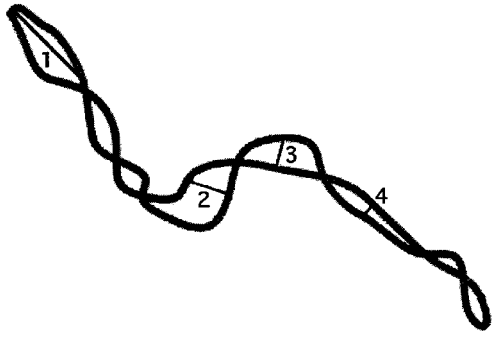

FIGURE 1 Sketch of a superhelical plasmid illustrating the superhelix diameter in the simulated conformations.

RESULTS AND DISCUSSION

Small angle neutron scattering measurements

The measured static form factor of the two plasmids p1868 and pUC18 shows the same Na^+ concentration dependent behavior. An undulation in the scattering curve at a momentum transfer $q = 0.5\ nm^{-1}$ present at 10 mM Tris, 0 mM Na^+ concentration shifts to higher q values with increasing Na^+ concentration. Fig. 2 shows the superposition of the measured scattering intensity of pUC18 between 0 and 500 mM Na^+ concentration. At 1 and 1.5 M the scattering curve superimposes with the curve at 0.5 M Na^+ (data not shown), there was no indication for any further structural change above 100 mM Na^+ concentration. The dependence of magnitude and position of the curve undulation on the Na^+ concentration is clearly visible in H_2O. However, the effect is more noticeable in D_2O because of the better signal-to-noise ratio at high q values. The scattering function of both superhelical plasmids at 0 and 100 mM Na^+ concentration, measured in D_2O, is shown in Fig. 3. The curve shape is identical for both plasmids, the change is slightly larger for pUC18. The largest decrease of the scattering intensity occurs at the same scattering vector for both plasmids.

To be sure that the observed change is not due to intermolecular interactions, i.e. not dependent on the DNA concentration, we collected data on pUC18 DNA at different concentrations in the range 2–6 mg/ml. The salt dependence of the scattering curves was not affected by the DNA concentration (data not shown). A detailed study on the effect of DNA concentration on the scattering curves had demonstrated that interference peaks begin to appear at concentrations greater than 20 mg/ml (Grassian et al., 1983). Moreover, the scattering curves of the relaxed form of pUC18 show no dependence on salt concentration (Fig. 4).

For quantifying the effect, we computed the ratio of the scattering intensities of the superhelical DNA at different salt concentrations and the relaxed form at 100 mM (Fig. 5).

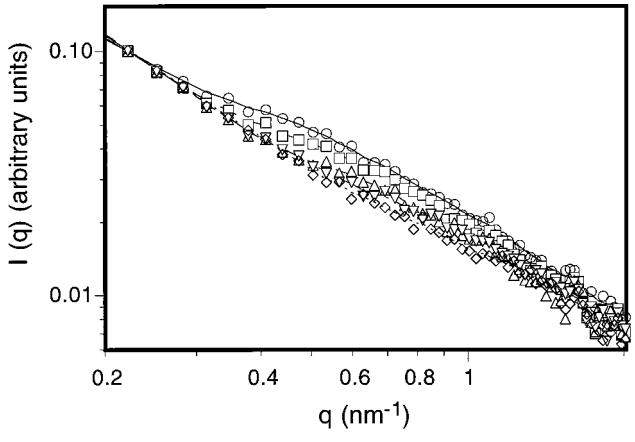

FIGURE 2 Measured scattering intensity $I(q)$ of pUC18, supercoiled, in H_2O, 10 mM Tris, at various Na^+ concentrations: 0 mM (○), 10 mM (□), 40 mM (△), 100 mM (▽), 500 mM (◇).

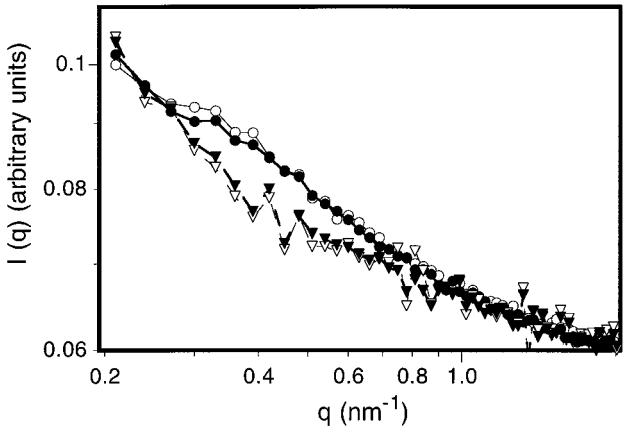

FIGURE 3 Measured scattering intensity $I(q)$ of pUC18 at 0 mM (○) and 100 mM (▽) and p1868 at 0 mM (●) and 100 mM (▼) Na^+ concentrations, both supercoiled, in D_2O, 10 mM Tris.

The shape of this curve is similar to the form factor of a pair of point scatterers at a constant distance d, $f_p(d, q) = [1 + (\sin(qd)/qd)]^2$ (solid lines in Fig. 5). This behavior is to be expected if a certain intramolecular distance occurs with high probability in the superhelical, but not in the relaxed DNA. The Debye formula for the scattering form factor of a macromolecule consisting of identical subunits is

$$P(q) = \frac{1}{N^2} \sum_{i=1}^{N} \sum_{j=1}^{N} \frac{\sin(q|\vec{r}_i - \vec{r}_j|)}{q|\vec{r}_i - \vec{r}_j|} f^2(q) \qquad (5)$$

where $f(q)$ is the q-dependent scattering form factor of the subunit (Cantor and Schimmel, 1980). We now compare two macromolecules A and B: A is a chain of point scatterers, B is the same chain but with pairs of point scatterers at a distance d arranged with their center of mass on the backbone of the chain. Thus, in Eq. 5 the coordinates $\vec{r}_i$ will be the same for the two structures, only $f(q)$ will be equal to 1 for structure A and equal to $f_P(d, q)$ for structure B. The ratio of the scattering intensities I_B/I_A will then be $f_P(d, q)$.

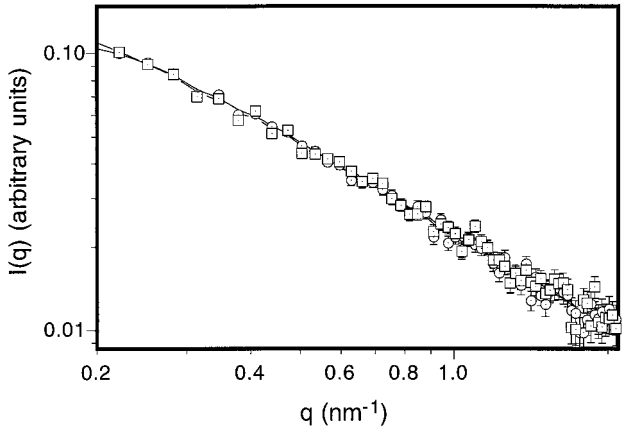

FIGURE 4 Measured scattering intensity $I(q)$ of pUC18, relaxed, in H_2O, 10 mM Tris, at 0 mM (○) and 100 mM (□) NaCl concentrations.

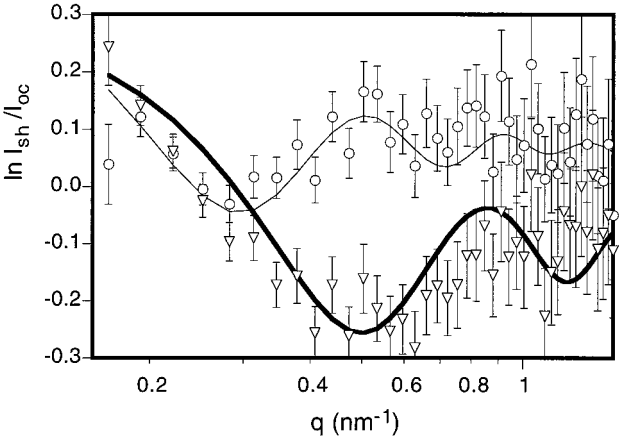

FIGURE 5 Ratio of the measured scattering intensities $I(q)$ of pUC18, supercoiled, in H_2O, 10 mM Tris, at 0 mM (○), and 100 mM (▽) Na^+ concentrations and relaxed pUC18 DNA at 100 mM Na^+ concentration. The *solid lines* are the scattering form factors of a pair of point scatterers at a distance $r = 16.0$ nm (*thin line*) and $r = 9.0$ nm (*thick line*).

In the case of a superhelical DNA where a certain intramolecular distance occurs with high probability we should find a very similar behavior.

We therefore concluded that the diameter of the superhelical regions of the DNA can be determined from a quantitative comparison of the NaCl-dependent scattering curves of superhelical DNA and the NaCl-independent scattering curve of relaxed DNA. To proceed, we fitted the form factor $f_P(d, q)$ multiplied by a scaling factor a, to the curves in Fig. 5. The fits yielded a value for a of the order of 0.5. The value of d, which can be regarded as the superhelix diameter, decreased from 16.0 ± 0.9 nm at 0 mM to 13.8 ± 1.1 nm at 10 mM, 11.5 ± 0.7 nm at 40 mM, 9.0 ± 0.8 nm at 100 mM. No further shift of r at 500, 1000, or 1500 mM NaCl was detected. We regard this as a direct measure of the interstrand separation in interwound regions of the DNA superhelix, since the curve undulation only appears in supercoiled DNA and intermolecular interference effects can be excluded.

DNA simulations

We assume in the following that the 10 mM Tris present in the buffer can be taken into account by additional 10 mM NaCl in the simulations. We therefore speak about salt concentration, which means 10 mM Tris plus added NaCl. The salt-dependent change in the static form factor was predicted in simulated scattering curves of pUC18 and p1868. The relative decrease in the scattering intensity from 10 mM to 100 mM salt concentration is of similar size as in the measured curves. The superimposed measured and simulated scattering curves of pUC18 and p1868 are shown in Figs. 6 and 7, respectively.

Since the simulated scattering functions agree very closely with the measured ones for both plasmids, we may conclude that the Monte Carlo simulation procedure is a

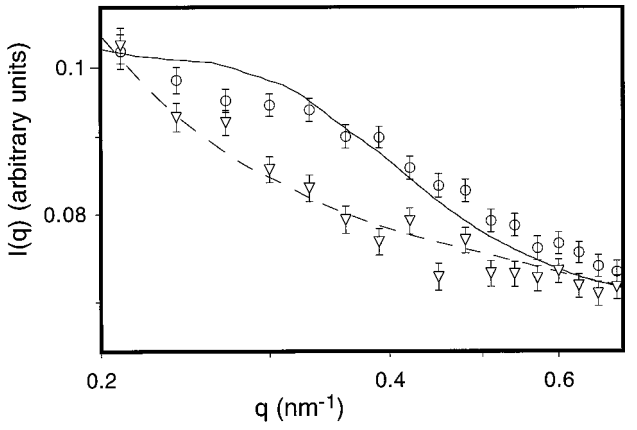

FIGURE 6 Measured and simulated scattering intensity $I(q)$ of pUC18, in D_2O, at 10 mM (exp., ○; sim., *solid line*) and 100 mM (exp, ▽; sim., *dashed line*) salt concentrations (NaCl + Tris).

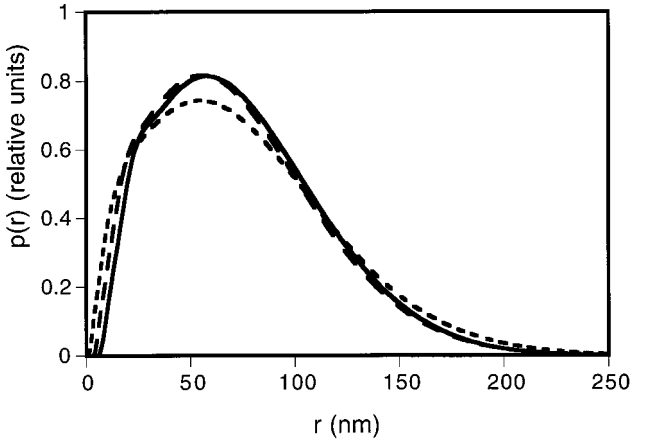

FIGURE 8 Distance distribution function $p(r)$ calculated from and averaged over the simulated configurations of pUC18, at 10 mM (——), 20 mM (— —), and 100 mM (. . . . . .) salt concentrations.

valid representation of the structure of superhelical DNA in solution. Thus, further calculations from the simulated conformations are possible, which reflect structural features of the DNA in free solution. We calculated the distribution function $p(r)$ of the distance r between all segment pairs of the DNA chain. The distribution was averaged over all conformations. The result for pUC18 is shown in Fig. 8. A sharp drop is seen for short distances which changes its position from ~20 nm at 10 mM to ~12 nm at 100 mM salt concentration. This cutoff can be used as a measure of the distance of closest approach for two segments in the superhelix. There was no significant further change of its position at higher salt concentration (data not shown).

To take a closer look at this cutoff, we calculated the average distribution function $p_n(r)$ of each segment $\vec{r}_i$ and its nearest neighbor $\vec{r}_j$ with the constraint that the two segments are separated by at least 10 segments along the chain. This function (Fig. 9) shows a pronounced peak which can be interpreted as the average superhelix diameter, its position at 18.0 ± 1.5 nm at 10 mM moves to 14.1 ± 1.5 nm at 20 mM and to 9.4 ± 1.5 nm at 100 mM salt concentration. The distribution was identical but with a shorter tail for the p1868 plasmid (data not shown). Again, there was no further significant change above 100 mM salt concentration.

The measured (Fig. 5) and simulated (Fig. 9) superhelix diameters are compared in Fig. 10. The agreement above 10 mM salt concentration is almost perfect. The same results were obtained for p1868. The superhelix diameters simulated for a 7-kb plasmid by Rybenkov et al. (1997) are shown for comparison in Fig. 10. They agree equally well with our experimental data, but they also show a small deviation at 10 mM. In the study by Rybenkov et al. (1997), the superhelix diameters were determined via a calculation of the superhelix pitch angle, the writhe and the number of superhelix ends from the simulated conformations. The deviation at low salt concentration in our study might be due to a change in the DNA persistence length, which has not been taken into account in the simulations. To check the

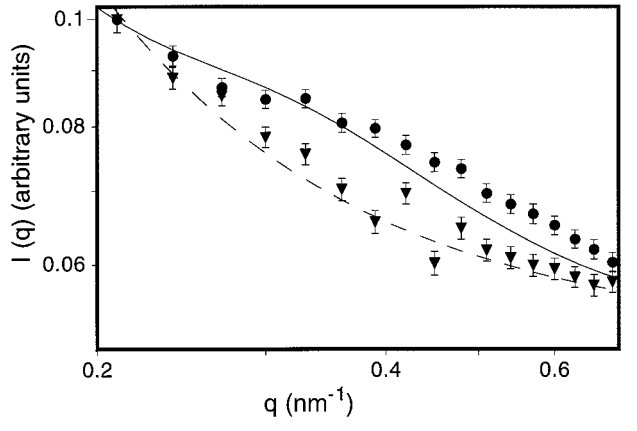

FIGURE 7 Measured and simulated scattering intensity $I(q)$ of p1868, in D_2O, at 10 mM (exp., ●; sim., *solid line*) and 100 mM (exp., ▼; sim., *dashed line*) salt concentrations (NaCl + Tris).

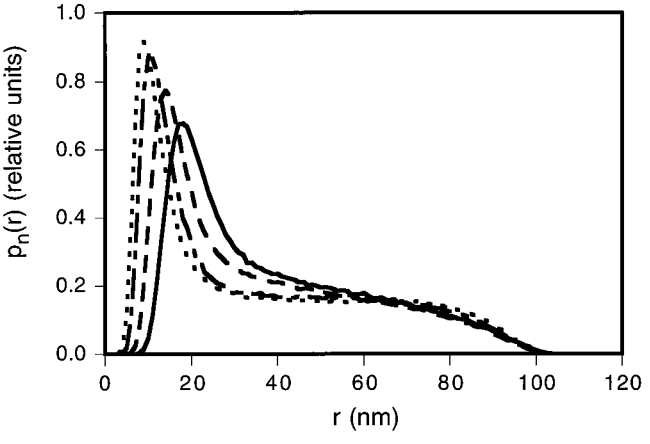

FIGURE 9 Distance distribution function $p_n(r)$ of the nearest neighbor of each segment, calculated from and averaged over the simulated configurations of pUC18, at 10 mM (——), 20 mM (— —), 50 mM (— - —), and 100 mM (. . . . . .) salt concentrations.

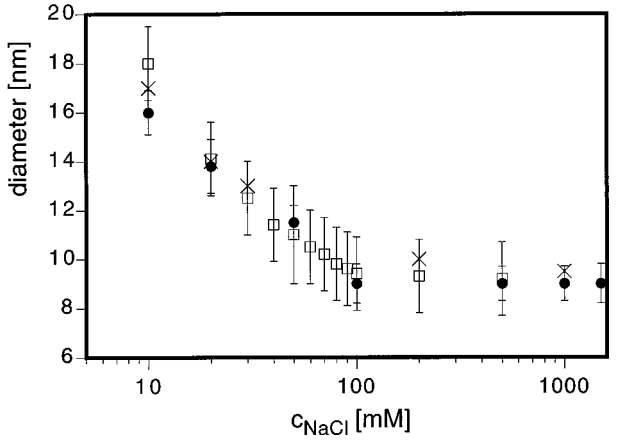

FIGURE 10 Measured (●) and simulated (□) superhelix diameter of pUC18 vs. salt concentration. The values calculated by Rybenkov et al. (1997) are shown for comparison (×).

influence of the persistence length, we performed a simulation of superhelical pUC18 DNA at 10 mM salt with a persistence length of 75 nm rather than 50 nm. The result was a dramatic decrease in the superhelix diameter. We obtained a value below 12 nm instead of 18 nm. Thus, the change in the persistence length at this low salt concentration is probably not that large, but it might be responsible for the small deviation of the simulated from the measured superhelix diameter. At 100 mM, the value agrees with the diameter of superhelical regions 9.2 ± 3.3 nm of p1868 as determined by scanning force microscopy in aqueous solution in the presence of 10 mM $MgCl_2$ and 30 mM NaCl (Rippe et al., 1997b).

However, the results contradict cryo-electron microscopy studies by Adrian et al. (1990), who found a superhelix diameter of 12 nm in 10 mM Tris which decreases to 4 nm by addition of 10 mM $MgCl_2$ and also puts into question the finding of a lateral collapse of the DNA superhelix (Bednar et al., 1994).

CONCLUSIONS

We have studied the salt concentration dependence of the superhelix diameter of two superhelical DNAs p1868 (1868 bp) and pUC18 (2868 bp). The static form factors of both plasmids were measured by small angle neutron scattering in aqueous solution. A significant decrease of the scattering intensity around the scattering vector $q = 0.5\ nm^{-1}$ with increasing salt concentration from 0 to 100 mM Na^+ in 10 mM Tris was detected. The effect occurred for both plasmids only in the supercoiled form and was independent of DNA concentration. At Na^+ concentrations >0.1 M, no significant change in the scattering curve could be found. Thus, similar to the recent findings of Gebe et al. (1996), a lateral collapse of the interwound structure for Na^+ concentrations >0.1 M, as observed by Bednar et al. (1994) in cryo-electron microscopy studies, is not supported by our data for superhelical DNA in free solution.

The experimental data can be quantitatively reproduced by Monte Carlo simulations. The superhelix diameter, which was here defined as interstrand separation in plectonemic regions of the chain, was calculated from the simulated conformations. It decreases with increasing salt concentration from 18.0 ± 1.5 nm at 10 mM to 9.4 ± 1.5 nm at 100 mM. In a recent study, similar values were obtained from MC simulations by a completely different calculation (Rybenkov et al., 1997). The value at high salt concentration is in agreement with previously reported diameters measured by scanning force microscopy in aqueous solution (Rippe et al., 1997b) and with earlier electron microscopy studies (Boles et al., 1990). The Monte Carlo simulation algorithm reproduces quantitatively the solution structure of DNA in solution. It is part of a combined Monte Carlo and Brownian dynamics algorithm. The Brownian dynamics part has already been shown to calculate correctly certain structural and dynamical features of superhelical DNA, e.g., the salt dependence of internal motions (Hammermann et al., 1997).

Parts of this work were supported by BMBF Grant 01KW9620 (to J.L.).

REFERENCES

Adrian, M., B. ten Heggeler-Bordier, W. Wahli, A. Z. Stasiak, A. Stasiak, and J. Dubochet. 1990. Direct visualization of supercoiled DNA molecules in solution. *EMBO J.* 9:4551–4554.

Bates A. D., and A. Maxwell. 1993. DNA Topology. Oxford University Press, Oxford.

Bednar, J., P. Furrer, A. Stasiak, J. Dubochet, E. H. Egelman, and A. D. Bates. 1994. The twist, writhe and overall shape of superhelical DNA change during counterion-induced transition from a loosely to a tightly interwound superhelix: possible implications for DNA structure *in vivo*. *J. Mol. Biol.* 235:825–847.

Boles, T. C., J. H. White, and N. R. Cozzarelli. 1990. Structure of plectonemically supercoiled DNA. *J. Mol. Biol.* 213:931–951.

Brady, G. W., M. Satkowski, D. Foos, and C. J. Benham. 1987. Environmental influences on DNA superhelicity: the effect of ionic strength on superhelix conformation in solution. *J. Mol. Biol.* 195:185–191.

Debye, P. 1915. *Ann. Physik.* 28:809–823.

Gebe, J. A., S. A. Allison, J. B. Clendenning, and J. M. Schurr. 1995. Monte Carlo simulations of supercoiling free energies for unknotted and trefoil knotted DNAs. *Biophys. J.* 68:619–633.

Gebe, J. A., J. J. Delrow, P. J. Heath, B. S. Fujimoto, D. W. Stewart, and J. M. Schurr. 1996. Effects of Na^+ and Mg^{2+} on the structures of supercoiled DNAs: comparison of simulations with experiments. *J. Mol. Biol.* 262:105–128.

Grassian, V., G. W. Brady, and C. J. Benham. 1983. X-ray conformational study of the DNA duplex in solution. *Biopolymers.* 22:1523–1543.

Hagerman, P. J. 1988. Flexibility of DNA. *Annu. Rev. Biophys. Biophys. Chem.* 17:265–286.

Hammermann, M., C. Steinmaier, H. Merlitz, U. Kapp, W. Waldeck, G. Chirico, and J. Langowski. 1997. Salt effects on the structure and internal dynamics of superhelical DNAs studied by light scattering and Brownian dynamics. *Biophys. J.* 73:2674–2687.

Kapp, U., and J. Langowski. 1992. Preparation of DNA topoisomers by RP-18 high performance liquid chromatography. *Anal. Biochem.* 206: 293–299.

Klenin, K., M. D. Frank-Kamenetskii, and J. Langowski. 1995. Modulation of intramolecular interactions in superhelical DNA by curved sequences. A Monte Carlo simulation study. *Biophys. J.* 68:81–88.

Klenin, K., H. Merlitz, and J. Langowski. 1998. A Brownian dynamics program for the simulation of linear and circular DNA and other wormlike chain polyelectrolytes. *Biophys. J.* 74:780–788.

Klenin, K. V., A. V. Vologodskii, V. V. Anshelevich, V. Y. Klishko, A. M. Dykhne, and M. D. Frank-Kamenetskii. 1991. Computer simulation of DNA supercoiling. *J. Mol. Biol.* 217:413–419.

Kremer, W., K. Klenin, S. Diekmann, and J. Langowski. 1993. DNA curvature influences the internal motion of superhelical DNA. *EMBO J.* 12:4407–4412.

Langowski, J. 1987. Salt effects on internal motions of superhelical and linear pUC8 DNA. *Biophys. Chem.* 27:263–271.

Langowski, J., G. Chirico, and U. Kapp. 1994. DNA supercoil dynamics studied by dynamic light scattering and Brownian dynamics simulations. *In* Structural Biology: The State of the Art. R. H. Sarma and M. H. Sarma, editors. Adenine Press, Schenectady, NY. 175–189.

Langowski, J., and U. Giesen. 1989. Configurational and dynamic properties of different length superhelical DNAs measured by dynamic light scattering. *Biophys. Chem.* 34:9–18.

Langowski, J., U. Giesen, and C. Lehmann. 1986. Dynamics of superhelical DNA studied by photon correlation spectroscopy. *Biophys. Chem.* 25:191–200.

Merlitz, H., K. Rippe, K. Klenin, and J. Langowski. 1998. Looping dynamics of linear DNA molecules and the effect of DNA curvature: a study by Brownian dynamics simulation. *Biophys. J.* 74:773–779.

Rippe, K., M. Guthold, P. H. von Hippel, and C. Bustamante. 1997a. Transcriptional activation via DNA-looping: visualization of intermediates in the activation pathway of E. coli RNA polymerase · s^{54} holoenzyme by scanning force microscopy. *J. Mol. Biol.* 270:125–138.

Rippe, K., N. Mücke, and J. Langowski. 1997b. Superhelix dimensions of a 1868 base pair plasmid determined by scanning force microscopy in air and in aqueous solution. *Nucleic Acids Res.* 25:1736–1744.

Rybenkov, V. V., A. V. Vologodskii, and N. R. Cozzarelli. 1997. The effect of ionic conditions on the conformations of supercoiled DNA. 1. Sedimentation analysis. *J. Mol. Biol.* 267:299–311.

Schellman, J. A., and D. Stigter. 1977. Electrical double layer, zeta potential, and electrophoretic charge of double-stranded DNA. *Biopolymers.* 16:1415–1434.

Schurr, J. M. 1977. Theory of dynamic light scattering by polymers and gels. *Chem. Phys.* 30:243–247.

Schurr, J. M., B. S. Fujimoto, P. Wu, and L. Song. 1992. Fluorescence studies of nucleic acids: dynamics, rigidities and structures. *In* Topics in Fluorescence Spectroscopy. J. R. Lakowicz, editor. Plenum Press, New York. 137–229.

Stigter, D. 1977. Interactions of highly charged colloidal cylinders with applications to double stranded DNA. *Biopolymers.* 16:1435–1448.

Vologodskii, A. V., S. D. Levene, K. V. Klenin, M. D. Frank-Kamenetskii, and N. R. Cozzarelli. 1992. Conformational and thermodynamic properties of supercoiled DNA. *J. Mol. Biol.* 227:1224–1243.